Acta Polytechnica **53**(2):197–212, 2013

available online at `http://ctn.cvut.cz/ap/`

MATERIALS FOR FUSION APPLICATIONS

Jiří Matějíček*

Institute of Plasma Physics, Prague, Czech Republic

* corresponding author: `jmatejic@ipp.cas.cz`

Abstract. An overview of materials foreseen for use or already used in fusion devices is given. The operating conditions, material requirements and characteristics of candidate materials in several specific application segments are briefly reviewed. These include: construction materials, electrical insulation, permeation barriers and plasma facing components. Special attention will be paid to the latter and to the issues of plasma-material interaction, materials joining and fuctionally graded interlayers.

Keywords: nuclear fusion, materials, plasma facing components, plasma-material interaction, functionally graded materials.

1. Introduction

Nuclear fusion is a potential source of relatively clean and safe energy for the future, and one of the very few options available to solve the looming energy crisis. It offers significant advantages over other large scale sources – in particular its inherent safety, cheap and abundant fuel and minimum radioactive waste [54]. Its technological realization is an extremely complex task, and as such is the subject of massive research activity in a broad international collaboration. Its success is critically dependent on the availability of materials able to function in harsh environments and on concurrent developments in plasma physics and control.

This paper reviews the material issues in fusion-oriented devices. First, the operating principle will be briefly reviewed, and technological realization illustrated on the ITER tokamak. Second, the materials–environment interactions will be introduced; specifically, these will concern the interactions with hot plasma, hydrogen isotopes and neutron irradiation. Third, particular materials in specific application sectors in a fusion device will be presented. These involve construction materials, plasma facing components, cooling system, electrical insulation, permeation barriers and breeding blanket systems. The issues related to the material joining will also be discussed. Finally, the material requirements for a future fusion reactor (DEMO) will be mentioned, together with candidate materials under development. While the topic of fusion materials is too broad for a comprehensive review in a single paper, some aspects will be treated on an introductory level. More focus will be given to plasma facing components and related issues.

2. Fusion, tokamak, ITER

The principle of nuclear fusion is the reaction of two light nuclei to form a heavier nucleus. Among reactions that release energy, the D−T reaction appears the most feasible to achieve on Earth:

$$\mathrm{D} + \mathrm{T} \longrightarrow \mathrm{He} + \mathrm{n}. \qquad (1)$$

The products carry the following energies: He: 3.5 MeV (used for further heating of the fuel), neutron: 14.1 MeV (used for energy production and tritium breeding). In order to achieve energy gain, a sufficient frequency of these reactions (collisions) has to take place. This translates into the requirement to keep the fuel at a sufficiently high temperature and concentration for a sufficiently long time (Lawson's criterion) [54]. The role of technology is to provide these conditions, especially plasma heating and plasma confinement. Two approaches are represented by inertial and magnetic confinement. There are two types of magnetic confinement devices – tokamak [96] and stellarator [95] – slightly differing in their geometrical arrangement. As the tokamak appears to be the most advanced concept today, only this application will be considered here.

Tokamak is a torus-shaped vessel that houses the hot plasma (temperatures are of the order of tens of millions °C) [96]. The plasma forms a single loop of the secondary circuit of a large transformer, which provides ohmic heating (Fig. 1). However, as the resistivity of plasma decreases with increasing temperature, the ohmic heating becomes ineffective, and additional means of heating are needed, e.g. radio frequency heating and neutral beam injection [96]. To confine the plasma to the center of the vessel, a set of magnetic coils of different orientation is applied, surrounding the vessel. A complex magnetic field keeps the plasma particles near the center of the torus, where they move along shallow helical trajectories. However, this cannot be done indefinitely, and after some time they reach the walls. The consequences will be discussed in the next section.

ITER is a large tokamak device, currently under construction in France [32]. While the existing large devices were oriented primarily towards scientific feasibility of fusion, the role of ITER is to verify the technological feasibility. In technical terms, its goals are to demonstrate extended burn of D−T plasma and to integrate and test the technologies and compo-

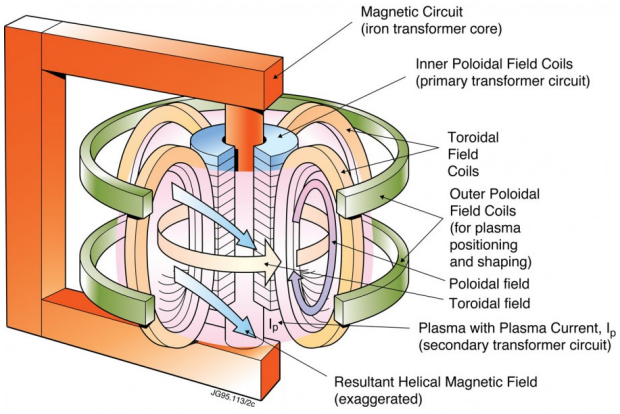

Figure 1. Schematic diagram of tokamak structure and operation; image courtesy of EFDA, www.efda.org.

nents essential for a fusion reactor as a source of energy. The next step device, called DEMO, should demonstrate the production of electricity and precede commercial power stations [54]. A cross-section of the core part of ITER is shown in Fig. 2. The vacuum vessel (light grey) provides the vacuum necessary to sustain the plasma, and a barrier for radioactive species. The plasma facing components absorb most of the heat and particle fluxes from the plasma. The first wall + blanket (full grey) makes up about 80 % of the plasma facing area; its role lies in neutron and thermal shielding (Be) and tritium breeding (Li). The latter function will be provided in full only in DEMO, while in ITER, only few test blanket modules will be used. The objective of the divertor (beige) is to exhaust helium and heat generated by the fusion reaction. The general overview of materials–environment interactions in such a tokamak device will be given in Section 3. Characteristics of specific materials for different application areas will be discussed in Section 4.

3. Materials in Fusion Environment

In a fusion reactor, materials will have to function in rather extreme conditions – they will be subjected to complex thermal, mechanical and chemical loads as well as strong irradiation (see Tabs. 1 and 2). Material properties will change as a result of elevated temperature and irradiation, component damage during service can be expected and repairs needed. Hence, the materials issues are quite complex, the materials are close to their limits, and new developments and alternatives are being sought.

3.1. Plasma–Material Interactions

Plasma–wall interaction is important for the choice of plasma facing materials and for the plasma scenarios compatible with material constraints [72]. The primary modes of interaction are two-fold. The plasma facing materials are subjected to heat and particle fluxes from the plasma. When these materials are eroded, particle emission back to the plasma takes place and influences the discharge. Under normal operation, ITER will generate about 500 MW of fusion power. Most of this energy will be carried by neutrons, only a smaller part by helium. Besides the steady-state operation, various transient events are expected to occur. These differ in frequency, duration and energy release, and are classified into three types: disruptions, vertical displacement events (VDE) and edge-localized modes (ELM). Disruption takes place when the stability limit is reached. The loss of confinement leads to thermal quench, when plasma particles having ∼10 keV energy are deposited within ∼ms time onto the plasma facing surfaces. The energy densities can reach 2 MJ m^{-2} on the first wall and 12 MJ m^{-2} on the divertor. During a current quench, the remaining energy of the magnetic field is deposited in the plasma, which intensely radiates, resulting in emitted energy densities up to ∼3 MJ m^{-2} during time period of the order of 10 ms. The peak energy densities can reach up to 20 MJ m^{-2}. Vertical displacement event is a slow drift of plasma column, leading to a contact with the wall, followed either by a disruption or a less severe loss of plasma thermal energy. The duration of this event can be $0.1 \div 1$ s; as a result, it affects the materials into greater depth, including joints. Edge-localized mode is a quasi-periodic (∼1 Hz), temporary relaxation of high plasma confinement (H-mode) that normally does not lead to discharge termination. It is associated with the loss of only few % of plasma energy, duration is several 100 µs, and can be also used for cleaning the plasma from impurities. All these transient events impose severe power loads on the material surfaces, strongly affecting their lifetime (see below). Therefore, developments towards improved plasma control are ongoing, aimed at disruption mitigation and reducing the severity of ELMs [72, 93].

When the energetic ions and neutral particles from the plasma impact on the plasma facing surface, the following processes may take place: erosion (by physical or chemical sputtering, flaking, melting, evaporation or arcing), absorption, chemical bonding and redeposition of the eroded material [33]. The amount of material eroded during a single disruption can be of the order of tens of µm. More specific erosion estimates for different cases are provided in [44, 26]. Some of the eroded material undergoes local redeposition, and only a fraction of it contributes to mobilizable dust [72]. If a combination of plasma facing materials is used, as proposed for ITER, this phenomenon leads to formation of mixed layers. This change in composition then brings about changes in the materials properties. Also, the extent of erosion and deposition varies with the location in the device, depending on the local plasma conditions and magnetic field [43]. The heat flux from the plasma causes a temperature rise of the surface which may lead to cracking, melting

Parameter	ITER	DEMO
Plasma current (MA)	$9 \div 17$	17
Plasma volume (m^3)	830	940
Fusion power (MW)	$350 \div 700$	3 000
Plasma temperature $\langle T \rangle$ (keV)	$8 \div 12$	17
Plasma density $\langle n \rangle$ ($10^{19}\,m^{-3}$)	$7 \div 12$	12
Total heating power (MW)	$120 \div 175$	660
Radiation power in edge and divertor (MW)	$60 \div 85$	390
Net operation length (days/year)	$5 \div 15$	280
Energy exhaust (GJ/day)	3 000	60 000
Max. gross material erosion rate at 1 % yield (mm/oper. year)	300	3 000
Tritium consumption (g/day)	20	1 000

TABLE 1. Selected general parameters of ITER and DEMO (compiled from [79, 67]).

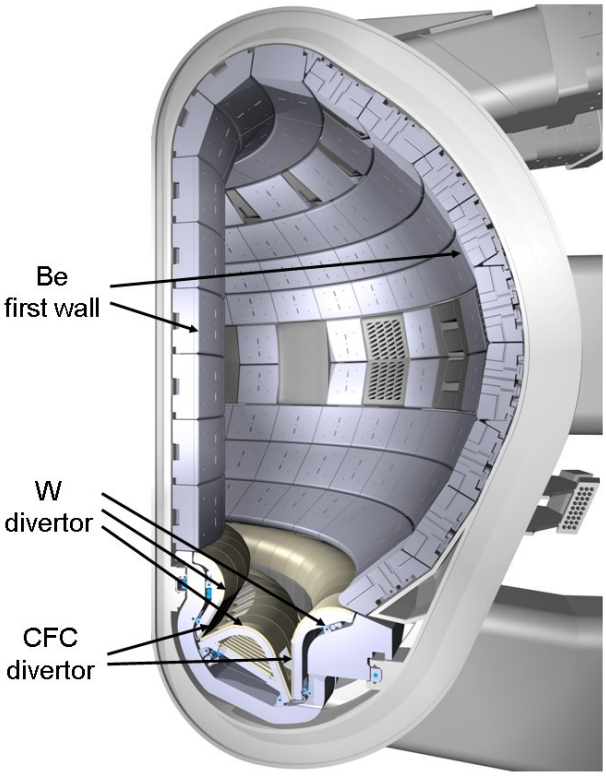

FIGURE 2. Cross section of ITER vacuum vessel and the plasma facing components (PFC); image courtesy of ITER, www.iter.org.

and/or evaporation or sublimation. The evaporated material may partially shield the surface, resulting in heat flux redistribution over a larger area [26, 6]. Still, the main mechanism of metallic armor damage is surface melting and melt motion caused by direct action of dumped plasma [6]. Temperature gradients lead to thermal stresses in the plasma facing components and stress concentration at the joints. The particles released to the plasma get ionized, the transitions are associated by electromagnetic radiation and cause radiation losses; these may terminate the discharge if too high.

All the above phenomena take place to a different extent in dependence of specific plasma facing material and position in the fusion device. Some will be treated in more detail together with the relevant materials in Section 4.2.

3.2. Interactions with Hydrogen Isotopes

The interaction of fusion materials with hydrogen isotopes is important from the point of view of the effects on materials properties and behavior, as well as for the fuel balance. The first wall in fusion devices is exposed to a high flux ($10^{20} \div 10^{24}\,m^{-2}\,s^{-1}$) of hydrogen isotopes (H, D and T), having energies from eV to keV [73]. These will diffuse through and dissolve in the exposed materials, to an extent depending on the material composition, structure and temperature. Examples of hydrogen diffusivity and solubility in various fusion materials can be found in [10]. A typical detrimental effect common to many metals is hydrogen embrittlement [94]. When the hydrogen atoms diffuse through the metal with high solubility, they may recombine in minuscule voids of the metal matrix and form hydrogen molecules. These then create pressure inside the cavity, up to levels where the metal has reduced ductility and tensile strength, and hydrogen induced cracking commences [94].

An important damage formation mechanism in tungsten is related to the low solubility of hydrogen in W. When exposed to a large flux of hydrogen isotopes, e.g. by D ion implantation, the D concentration in the implantation zone exceeds the solubility limit and stresses the crystal lattice until plastic deformation alleviates these tensions. Plastic deformation of the W matrix caused by deuterium super-saturation within the near-surface layer can then result in bubble and void formation [73].

Helium, besides being present as a product of the fusion reaction, can be also generated by transmutation reactions in amounts ranging from less than one to thousands of atomic parts per million (appm), depending on the neutron spectrum, fluence, and alloy composition [15]. It has to some extent similar effects

Table 2. Operational conditions of plasma facing components in ITER and DEMO (compiled from [7, 8, 1, 67, 31]); the numbers presented in Tables 1 and 2 should be taken as approximate/projected only, since both devices are still to be built, alternative design concepts exist, and future plasma behavior can be only estimated to a certain degree.

	ITER		**DEMO**	
	First Wall	Divertor	First Wall	Divertor
Component replacements	none	up to 3	5 year cycle	5 year cycle
Avg. neutron fluence (MWa/m^2)	0.3	<0.15	10	5
Displacement damage/ transmutation production (dpa/appm He) or (dpa/% Re for W)	Be 1/1000 Cu 3/30 SS 3/30	CFC 0.7/230 W $0.5 \div 0.7/0.15$ % Re Cu 1.7/16 SS1.6/16	W 30/6 % Re RAFM $100 \div 150/1200$	W 15/3 % Re RAFM $20 \div 60/600$
Normal operation				
No. of cycles	30 000	10 000	< 1000	< 1000
Incident plasma temperature (eV)			$100 \div 500$	$500 \div 1000$
Peak particle flux ($10^{21}/m^2s$)	1	~ 1000	2	$500 \div 1000$
Surface heat flux (MW/m^2)	< 0.5	$3 \div 10$	< 1	$10 \div 20$
PFM operational temperature (°C)	Be $200 \div 300$	W $200 \div 1000$ CFC $200 \div 1500$	W $550 \div 800$	W water coolant $500 \div 900$ W He coolant $650 \div 1450$
Coolant temperature (°C)		100 (water)		$600 \div 700$ (He)
ELM energy density (MJ/m^2)	-	< 1	$\ll 1$	$\ll 1$
ELM duration/frequency	-	0.2/∼Hz	-	infrequent
Off-normal operation				
Peak energy density (MJ/m^2)	60 (VDEs)	30 (disr.)	-	30
Duration (ms)/Frequency (Hz)	300/1 % (VDEs)	1-10/< 10 % (disr.)	-	$1 \div 10$

on materials as hydrogen isotopes. However, the accumulation of helium in metallic materials, especially tungsten, is more harmful than hydrogen because its strong interaction with defects. Helium enhances the formation of bubbles, leading to local swelling and degradation of mechanical properties [87].

The retention of hydrogen species in the fist wall is also an important issue. In particular, if large amounts of T are retained in the materials, this represents a large radioactive inventory after shutdown of the device, posing safety hazards. The safety limit for ITER is considered around 700 g [71]. In addition, T is part of the fuel that needs to be supplied by breeding from Li in the blanket and its retention of T in the first wall would degrade the fuelling efficiency. Therefore, the first wall material should retain as little hydrogen as possible. From the initial material combination for ITER (Be, C, W), tungsten is the most favorable candidate, especially because of its low solubility for hydrogen. The actual amount of hydrogen that can be retained in the material is determined by the defect density [73]. The defects act as trap sites for hydrogen where it is retained after exposure to the plasma, while the solute hydrogen diffuses out of the material. Intrinsic defects encompass grain boundaries, pores and inclusions, dislocations or thermal vacancies. Their concentration can vary depending on material grade and purity, thermal treatment and surface preparation. This natural defect density can be increased by radiation damage caused by the incident hydrogen ions and by the fast neutrons from the fusion reaction. These defects include Frenkel pairs, stress-induced dislocation networks, gas bubbles and damage clusters. While the damage by ions is limited to the near-surface regions, the neutrons produce trap sites throughout the bulk, thereby enhancing the potential for hydrogen retention. The density of irradiation-induced defects will generally decrease with temperature, by increased rate of spontaneous annihilation and vacancy clustering, while tritium can be released from weak traps [73].

An important aspect concerning carbon-based materials is chemical sputtering. Carbon reacts easily with hydrogen isotopes, forming (gaseous) hydrocarbons. Their volatility greatly enhances the erosion yield. The chemical sputtering yield of carbon is slightly larger for deuterium than hydrogen [25]. Codeposition of the eroded carbon leads to retention of hydrogen isotopes on materials that would otherwise be less sensitive to this issue. The re-erosion of these deposited layers exhibits about 10 times higher yield than on unaffected surfaces [71].

Overall, the tritium retention decreases in the following order: C, Be, W [72]. Estimates for tritium retention indicate that the abovementioned safety limit would be reached after ~ 500 discharges for this material combination, whereas this number would reduce to < 150 for an all-C surface. On the other hand, for a Be first wall and W divertor, some 3000 discharges can be expected. For an all-W surface, these estimates increase to >3000 and $\sim 15\,000$, respectively, with and without neutron irradiation [71]. This aspect influences the material choice for ITER as well as future fusion devices, as will be further discussed in Sections 4.2 and 5.

Besides the materials choice, procedures for tritium recovery and for mitigation of tritium retention are sought. Potential schemes under consideration include optimization of the tritium fuelling efficiency, tailoring the isotope ratio, seeding the divertor plasma with nitrogen and wall conditioning, e.g. by a low pressure radio-frequency discharges in deuterium [71]. Periodic cleaning (detritiation) will also be necessary. Possible techniques are baking in oxygen at high pressure, surface heating using scanning lasers or flash-lamps under remote handling, particularly for carbon-based materials and co-deposits. For tungsten and beryllium, thermal desorption at moderate temperatures may be sufficient [71].

3.3. Irradiation Effects

As mentioned above, the materials in the vicinity of the plasma are subjected to significant flux of energetic ions and, in the case of fusion reactor, neutrons. Radiation damage occurs as a result of the interaction of incident particles with the atoms in the target material. This interaction depends on the mass, electrical charge and energy of the incident particles, as well as on the characteristics of the target material. During this interaction, the incoming particles lose their energy in the crystal through a) inelastic interactions with the target electrons, leading to ionization and/or excitation and then to electronic losses, and b) elastic collisions with the target nuclei, leading to atomic displacements, thereby forming vacancies and interstitial atoms (Frenkel pairs) [1]. At high enough energies, this process is repeated, and the displacement cascades can form larger damaged zones. The incoming particles can also be captured by the target nuclei, leading to nuclear transmutations and generation of impurities such as helium and/or hydrogen gas atoms.

The defects thus generated can a) recombine, b) diffuse through the material, c) annihilate at sinks, such as dislocations, grain boundaries, interfaces, d) cluster, either among themselves or with solute atoms, forming more complex secondary defects. The radiation damage can be to some extent counteracted by thermal annealing. The final microstructure then depends on the initial composition and microstructure of the material, on the irradiation conditions, as well as on the temperature of the material under irradiation. It may encompass a variety of secondary defects, such as small defect clusters, dislocation loops, stacking fault tetrahedra, precipitates, voids and/or helium bubbles. These microstructural changes lead to changes in dimensions, chemical composition on a microscale, physical and me-

chanical properties. These changes are generally for the worse, and may include a decrease in electrical and/or thermal conductivity, hardening, loss of ductility, loss of fracture toughness and/or loss of creep strength, loss of dimensional stability (especially volume increase – 'swelling'), among others. In addition, the irradiated material may become radioactive, due to nuclear transmutation reactions.

Irradiation effects are strongly dependent on temperature. The following examples are provided as typical for steels, considered as main structural materials:

- low temperatures, < 400 °C: strong embrittlement, increase in the ductile-to-brittle transition temperature (DBTT),
- intermediate temperatures, $300 \div 600$ °C: peak in swelling,
- higher temperatures, > 600 °C: irradiation-enhanced precipitation and creep effects [1].

In the case of tungsten, the presence of high energy neutrons in the fusion spectrum leads to formation of rhenium and osmium, with a strong influence on thermal and electrical conductivity, closely correlated with each other [5]. Irradiation to 4 dpa resulted in 24 % decrease in electrical conductivity. Thermal conductivity at 5 % Re content is 20 % lower than for pure W. Thermal conductivity changes after irradiation of various W−Re alloys were found to depend on composition and temperature, including opposite signs [22]. Tungsten is also susceptible to low-temperature embrittlement at $T < 0.3\,T_{\mathrm{m}}$, the causes of which are point defect generation, impurity segregation to grain boundaries and radiation-enhanced precipitation [39]. The strengthening of the metal matrix can raise the deformation stress to magnitudes higher than the cleavage strength of the alloy, resulting in brittle failure. While the addition of Re increases its ductility at elevated temperatures in the unirradiated state, this does not hold for irradiated materials [39].

Irradiation effects in ceramics are generally more complex than in metals. Ceramic materials contain more species, which can form a sublattice in the crystal. The threshold energy for atomic displacement can differ for each sublattice and may also depend on the crystal orientation [100]. Besides, ceramic materials are sensitive to radiation with lower energy than needed for atomic displacement by elastic collisions, especially ionizing radiation [100, 57]. In insulators in general, energy transfer by excitation of electrons is more significant than by atomic displacements [77]. The electrical insulation ability is rather sensitive to impurities, and as such is influenced by nuclear transmutations. The irradiation effects on electrical properties can be classified as follows:

- RIC – radiation-induced conductivity – transient increase in conductivity during the irradiation,
- RIED – radiation-induced electrical degradation – permanent increase of electrical conductivity, caused by defects formed by simultaneous influence of irradiation and electric field,
- surface effects,
- RIEMF – radiation-induced electromotive force, generated in metallic parts separated by an insulator [78, 17].

In specific ceramic materials, radiation-induced changes in thermal conductivity [82, 98, 27], mechanical [27] and optical properties [29] were also observed. These changes may happen even at very low dpa levels [82].

So far, all irradiation testing of candidate materials is performed using neutrons from fission reactors or a mixture of high-energy protons and spallation neutrons, whose energy spectra are somewhat different from those of a fusion reactor [90]. For improved relevance, a dedicated facility is planned – The International Fusion Materials Irradiation Facility (IFMIF) [19]. Currently in the design phase, it will be an accelerator-driven source of neutrons, using a stripping reaction between deuterium and lithium. Its objective is to produce an intense flux of neutrons with a broad peak near 14 MeV, in order to generate material and subcomponent irradiation test data characteristic to future fusion reactors. The IFMIF project is by some regarded as comparable to ITER, both in significance and cost [1].

4. Specific Materials and Applications

4.1. Construction Materials

The issues for the selection of structural materials relate to their physical, mechanical, chemical and neutronic properties. These materials have to function at elevated temperatures, be able to withstand high thermal stress, should be resistant to radiation damage, possess good compatibility with the coolants and other materials, long lifetime, high reliability, sufficient primary resources, easy fabrication and good safety and environmental behavior [1]. In particular, the performance requirements at high elevated temperatures translate to a small coefficient of linear expansion, high thermal conductivity and high ultimate tensile strength. Safety and environmental aspects dictate mainly low specific radioactivity, low radioactive decay heat, small half-life radionuclides, controlled paths for dispersion of radioactivity, reduced biological hazard potential and easy waste disposal. From the latter points, it follows that candidate structural materials for fusion reactors must have a chemical composition based on low activation chemical elements. These elements are very few: Fe, Cr, V, Ti, W, Si and C [1].

For ITER, where the requirements are less stringent, stainless steel 316LN is planned as the main construction material, resistant to long term irradiation, mechanical loading and contact with water. A variety of components can be provided by hot or cold rolling, bending, forging, or extrusion, and can be also

available as casting grades [52]. For DEMO, reduced activation ferritic/martensitic steels, vanadium-based alloys, fibre reinforced SiC−SiC ceramic composites and tungsten-based materials are considered [1], see also Section 5.

4.2. Plasma Facing Materials

General requirements

The main criteria for the selection of plasma facing materials are the plasma parameters (ion and neutron fluxes, temperature) and the heat flux in particular location, erosion and expected lifetime, emission of impurities into the plasma and radiation losses, tritium retention, mechanical and thermal properties. The favorable characteristics are compatibility with the plasma and the underlying materials, high temperature stability, high erosion resistance, high fracture toughness and thermal shock resistance, high thermal conductivity, low irradiation changes and low tritium retention [33, 44, 7]. Since all of these cannot be satisfied by a single 'optimum' material, compromises have to be made, also taking into account the spatial variation of heat and particle fluxes from the plasma.

The initial material selection for ITER, i.e. beryllium on the main vessel walls, tungsten on the divertor upper baffle and dome, and carbon fibre composite around the strike points on the divertor plates, results mainly from plasma wall interaction considerations (to optimize a reasonable lifetime of the plasma facing components under a variety of plasma operational scenarios) [71, 72]. For the activated phase of ITER, a combination of W divertor and Be first wall is proposed, motivated by minimization of the T inventory. All-W surface is considered at a later stage in ITER, when full power $Q = 10$ discharges are established and reactor conditions are investigated [62, 72].

Beryllium

Beryllium is foreseen as the plasma facing material for the first wall of ITER and as a neutron multiplier material in solid breeder blankets. Among its advantages are lower Z number than carbon, oxygen gettering, absence of chemical sputtering, ability for in-situ repair by plasma spraying, etc. Disadvantages include its low melting temperature and high vapor pressure, high physical sputtering yield, mechanical property degradation during neutron irradiation, chemical reactivity with steam and relatively slow tritium release kinetics [14, 75]. As a plasma facing material, it has been already applied in three tokamaks [20]. When irradiated by neutrons, the nuclear reactions produce helium and tritium, which may be trapped at defects or precipitate as gas bubbles. These defects will increase the retention of hydrogen, by increasing the concentration of sites where diffusing hydrogen can precipitate as gas or become trapped as atoms [20]. Due to its toxicity and difficult handling, the number of laboratories able to process beryllium is very limited. For the plasma facing components, it can be applied either as bulk tiles, bonded to the heat sink, or as thick plasma sprayed coatings; the latter technique also offering the possibility of easy repair of damaged parts [30, 50, 20].

Carbon-based materials

In ITER, carbon-fibre composites (CFC) are foreseen for the divertor areas with the highest heat fluxes. The CFC consists of 3D structure of carbon fibres in a carbon matrix. As a result, the material is anisotropic, particularly in thermal conductivity and thermal expansion. These composites typically have higher strength and elastic modulus, and thus a superior performance under thermal stress and thermal shock. Another key advantage of these materials stems from the fact that they tend to fail in a less abrupt manner than homogeneous graphite or ceramics in general, due to the presence of the reinforcing fibers, which bridge evolving cracks [83]. An overview of thermophysical properties of several CFC types as well as graphite is provided in [83]. Among other advantageous characteristics are low Z, high heat flux resistance, the absence of melting and resistance to irradiation swelling. Irradiation, however, reduces its thermal conductivity, and therefore leads to increased thermal erosion during disruptions. Among the disadvantages of carbon-based materials are chemical erosion (as discussed in Section 3.2) and tritium absorption, especially during codeposition. The chemical erosion can be somewhat reduced by the addition of B, Si and other dopants [83]. The primary concern over retention of fuel in the PFC is the inventory of hydrogen adsorbed in the graphite or CFC and the subsequent release of near-surface hydrogen (due to physical or chemical sputtering, etc.) during plasma discharges. The hydrogen sputtered from the wall oversupplies the plasma edge with fuel, causing instabilities and problems with plasma control [83]. CFCs have been found to have an order of magnitude lower tritium retention than graphite, over a large range of irradiation doses [9].

The use of graphite-based materials, particularly CFCs, in ITER divertor is considered advantageous for the first phase of ITER operations, because CFCs have already demonstrated good performance in the currently operational facilities (e.g., Tore Supra). In the case of additional heating and off-normal events, which will be very likely during initial operation of ITER, the potential damage to the divertor components would be less serious for CFC than its primary 'competitor', tungsten [83].

Tungsten

Tungsten is one of the two candidate materials (with CFC) for the ITER divertor, namely for the areas with a high concentration of neutral particles [16] and the main candidate material for the next step device, DEMO [7]. Tungsten has the highest melting point of all metals, the lowest vapor pressure, good thermal conductivity and high temperature strength;

also, it does not form hydrides or codeposits with tritium [16, 80]. It has much higher atomic number than carbon or beryllium, which makes it a highly undesirable impurity in the plasma because of the radiation losses. On the other hand, it has also much higher threshold energy for sputtering, largely due to its high atomic weight. Among its disadvantages are the ductile-to-brittle transition, embrittlement under neutron irradiation, difficult machining and welding [50]. A comprehensive summary of relevant properties of tungsten and its alloys is provided in [80].

Research activities are directed towards improvements in tungsten's thermal conductivity, high temperature strength and stability, recrystallization temperature and ductility for operation under neutron loading. The investigations made during the recent years have shown that creep strength and recrystallization can be improved with only little effect on thermal conductivity by the use of dispersed oxides (e.g. La_2O_3, Y_2O_3), which stabilize the grains. The intrinsic brittleness of tungsten, however, cannot be improved by oxide dispersion [69]. Towards improvement in ductility, various powder metallurgical fabrication routes were followed, including mechanical alloying and hot isostatic pressing and/or hot/cold forming; the investigated materials being pure W, W−Ti, W−V and W−Ta alloys, in some cases reinforced with Y_2O_3, La_2O_3, or TiC particles. The important aspect is to form and retain small crystal grains. A prospective concept to enhance fracture toughness of tungsten is the use of tungsten-fiber reinforced tungsten composites, fabricated by chemical vapor infiltration [18]. The toughening mechanism is the so-called pseudo-toughness: a controlled crack deflection at the engineered fiber/matrix interfaces leads to internal energy dissipation by interface debonding and friction.

For tungsten, oxidation protection coatings are also being developed. The underlying event is the so-called 'loss of coolant accident', which would be associated with air ingress into the reactor vessel. This would lead to a temperature rise, tungsten oxidation and the release of volatile radioactive tungsten oxides. A possible way to avoid this important safety issue is the addition of oxide forming alloying elements to tungsten, leading to the formation of a self-passivating layer at high temperature in presence of oxygen. A good performance of W−Cr−Si coatings manufactured via magnetron sputtering was demonstrated, with even more promising results obtained on W−Cr−Ti alloys [37]. Studies on coatings were extended to bulk alloys as well [42].

The combination of plasma facing materials, their erosion and redeposition brings about issues related to compositional changes. For example, Be deposited on W may lead to the formation of Be_2W already at low temperatures ($\sim 130\,^{\circ}\mathrm{C}$) which has a reduced melting point of $\sim 2250\,^{\circ}\mathrm{C}$ [62]. Tungsten materials covered with a mixture of W and C or oxidized on the surface will have different sputtering threshold than pure tungsten. Increased D retention was also found in these cases [61]. Beryllium deposited on carbon has a favorable effect to reduce tritium retention compared with pure carbon [79]. Beryllium carbide formed on the surface of a carbon sample has been shown to correlate with the reduction of chemical erosion of the carbon surface [20]. Be_2C formed on Be surface is stable up to high temperatures and reduces the sputtering compared to pure Be. On the other hand, WC formed on W surface dissolves upon exposure to higher temperatures, and the sputtering is then similar to pure W [40].

4.3. Heat Sink

The ITER's cooling system should be capable of removing a heat flux exceeding $25\,\mathrm{MW\,m^{-2}}$. For this application, copper-based materials are planned, chiefly because of their high thermal conductivity. As pure copper does not show sufficient strength at higher temperatures, dispersion strengthened and precipitation strengthened materials are being developed. Of the latter, CuCrZr is the main candidate for ITER. Initially an alloy with $0.6 \div 0.9\,\%$ Cr and $0.1 \div 0.2\,\%$ Zr, It undergoes heat treatment to induce the precipitates that strengthen it [41]. The issues related to this material include irradiation hardening or softening, in dependence on temperature, creep at higher temperatures, problems with joining (thermal sensitivity); see also Section 4.4.

4.4. Materials Joining

The complex construction of a fusion device requires a variety of materials to be joined. This presents serious technological challenges, associated with the difference in materials properties (thermal, mechanical), resulting in stress concentration at the joint upon loading, poor wetting or mutual reactivity, neutronics limitations on brazing materials, etc. [49, 60]. Examples of these issues follow. CuCrZr material for the heat sink is thermally sensitive. When (plasma facing or construction) materials are joined to CuCrZr at higher temperatures, precipitate growth or dissolution may occur. During Be + Cu joining, high reactivity of Be even at moderately increased temperatures may lead to the formation of brittle intermetallics. In W + Cu joints, large difference in thermal expansion (higher for Cu) and elastic moduli (higher for W) causes large stresses at the interface upon heat loading. Similar problem is faced in CFC+Cu joints (CFC has lower modulus), where another challenge lies in poor wettability of CFC [55].

The available joining techniques include brazing, welding, hot isostatic pressing, pulse plasma sintering, active metal casting, explosion joining, diffusion bonding, etc.

Among the approaches to overcome the challenges mentioned above are the following:

- bonding at lower temperatures and/or shorter times, to avoid intermetallics formation or effects on the precipitates [4],
- third-material bonding interlayers, to prevent chemical reaction in some cases [28, 49], or show increased chemical affinity or improved wetting [34], provide a compliant layer for stress reduction [99], etc.,
- composites and graded layers (FGM), consisting of the two materials to be joined (with or without another material), to replace a sharp interface with a smooth transition, and reduce the stress peak (see below),
- different geometrical configurations of the surface relief (for mechanical interlocking) [30, 49] or the armor (e.g. castellation/macrobrush, for improved strain tolerance) [60, 6, 63].

The graded interlayers have been shown to reduce the maximum strain singificantly [56, 65]; the reduction is generally larger the thicker is the graded layer [91]. Several techniques have been explored for the production of composites and graded layers, such as plasma spraying [46], pulse plasma sintering [70], resistance sintering [92], laser cladding [64] etc. A brief assessment of different aspects of their applicability in plasma facing components of fusion reactors is provided in [91].

The plasma spraying technique offers the following advantages: easy formation of composites and FGMs with control of the compositional profile, possibility to provide a full change of material from one side to another (e.g. from 100 % Cu to 100 % W on the surface), thus eliminating the need for further joining, possibility of repairing damaged parts, ability to coat large areas (even non-planar surfaces), thickness range from ∼100 µm to several mm, significant strain tolerance [50]. The main drawback of plasma sprayed layers is their low thermal conductivity, originating in the lamellar structure with imperfect bonding between the layers [46, 89]. Example of W + Cu FGM produced by water stabilized plasma spraying is shown in Fig. 3. Several methods of post-treatment, aimed at conductivity improvement, were explored – hot isostatic pressing, copper infiltration, laser surface remelting [47], see Fig. 4. While a marked improvement in thermal conductivity was achieved, the applicability of these techniques for PFC fabrication is probably rather limited. Plasma sprayed tungsten-based coatings have shown moderate performance in high heat flux tests [51], but their low thermal conductivity precludes them from use in the divertor areas of ITER with the highest fluxes. However, they may still be applicable to the first wall of DEMO, where lower heat fluxes are expected (see Section 5).

4.5. Electrical Insulators

Electrical insulation materials are needed in the following areas: insulation of the vessel, diagnostics and auxiliary instruments, and the breeding blanket. For the vessel insulation, the main requirement

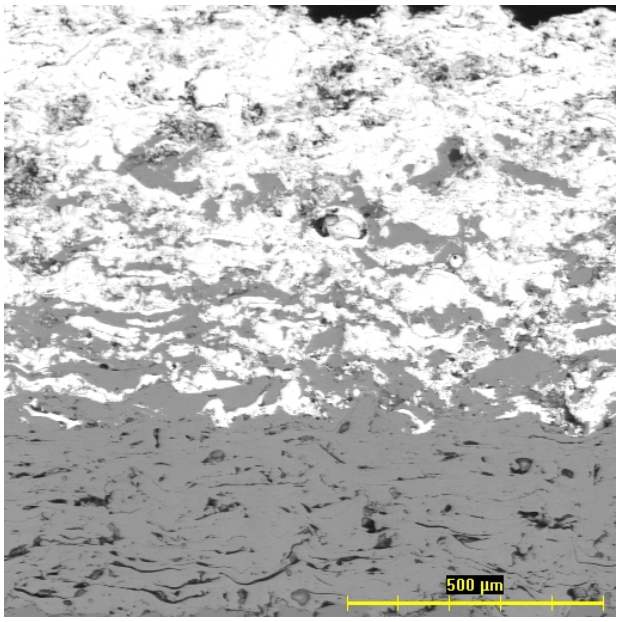

FIGURE 3. $W^{+}Cu$ FGM produced by water stabilized plasma spraying (SEM image in BE mode; dark grey – copper, light grey – tungsten).

(apart from dielectric properties) is mechanical stability. For this purpose, oxidic ceramics (e.g. Al_2O_3, $MgAl_2O_4$) are used, especially those manufactured by plasma spraying [49]. For the diagnostic components, stability in vacuum is also required. Both oxidic and non-oxidic ceramics and glasses are used. Changes in electrical, optical and mechanical properties with irradiation, as outlined in Section 3.3, have to be considered as well [17]. Electrical insulators in the breeding blanket will have to serve more complex functions, therefore will be treated separately in Section 4.7.

4.6. Permeation Barriers

As indicated in Section 3.2, permeation of hydrogen isotopes through structural materials is an important issue because of its safety and operational implications. This concerns mainly the breeding blanket, but also the plasma facing components. The considered structural materials typically have very high hydrogen permeability; this could be reduced by thin surface layers acting as permeation barriers. Such coatings have to fulfill the following requirements [81, 85]:

- TPRF >1000 in a gas-phase and TPRF >100 in a liquid breeder (where TPRF is the tritium permeation reduction factor, comparing the permeation through coated and bare structural material),
- compatibility with the Li-based breeder, high corrosion resistance,
- high thermomechanical integrity,
- self-healing (regeneration of the damaged barrier through in situ oxidation),
- applicability to large engineering components.

Permeation barriers should be made from materials having low diffusivity and/or low surface recombination constants. Among the prospective candidates are oxides, nitrides and intermetallics, such as Al_2O_3, Er_2O_3, $Cr_2O_3{-}SiO_2$, Fe_3Al and Fe_2Al_5 and others [49, 10]. The available techniques include hot-dip aluminizing (HDA), CVD, precipitation from liquid metals, ion implantation, cementation, chemical densification coating (CDC), thermal spraying, metallic coating with oxidative heat treatment, natural oxide growth from the gas phase, etc. [49]. Since hydrogen diffusion in materials is often governed by imperfections, high-quality coatings without significant void fractions or impurity contents are required [36]. The occurrence of cracks is often related to a difference of thermal expansion from the base material [10]. The ability to coat internal surfaces is also an important aspect for the selection of the coating technique [49]. While a number of techniques and material combinations have shown very high TPRF, there is significant evidence that the effectiveness of the permeation barriers decreases with irradiation, and, therefore, the good results may not necessarily be reproduced in a reactor environment [10].

4.7. Blanket Materials

The breeding blanket represents the most complex application, since it will have to integrate a number of materials to perform several functions, all in a severe environment. It has three main functions: a) to absorb the 14 MeV neutrons and transform their energy to provide most of the reactor power output, b) to provide neutron multiplication and breeding of tritium to fuel the reactor, at a rate equal to tritium consumption in the plasma plus losses in the reactor components, c) to shield the superconducting coils and the other external components [1, 24]. The tritium breeding will happen through a combination of these reactions [84]:

$$^{6}\mathrm{Li} + \mathrm{n} \longrightarrow \mathrm{He} + \mathrm{T}\ (4.78\,\mathrm{MeV}), \tag{2}$$

$$^{7}\mathrm{Li} + \mathrm{n} \longrightarrow \mathrm{He} + \mathrm{T} + \mathrm{n}'\ (-2.47\,\mathrm{MeV}). \tag{3}$$

The second reaction is beneficial in providing another neutron, but has negative energy balance; therefore, the ratio of the two Li isotopes has to be carefully optimized. Neutron multiplication can be achieved in beryllium as well:

$$^{9}\mathrm{Be} + \mathrm{n} \longrightarrow 2\,\mathrm{He} + 2\,\mathrm{n}'. \tag{4}$$

In both cases, slight oversupply has to be provided to ensure self-sufficiency, the reasons being that a) not all of the surface surrounding the plasma will be covered by the blanket, and b) some portion of the reaction products will be absorbed by the neighboring components. The measure of this self-sufficiency is called the tritium breeding ratio (TBR) and its value is dependent of specific design parameters [23].

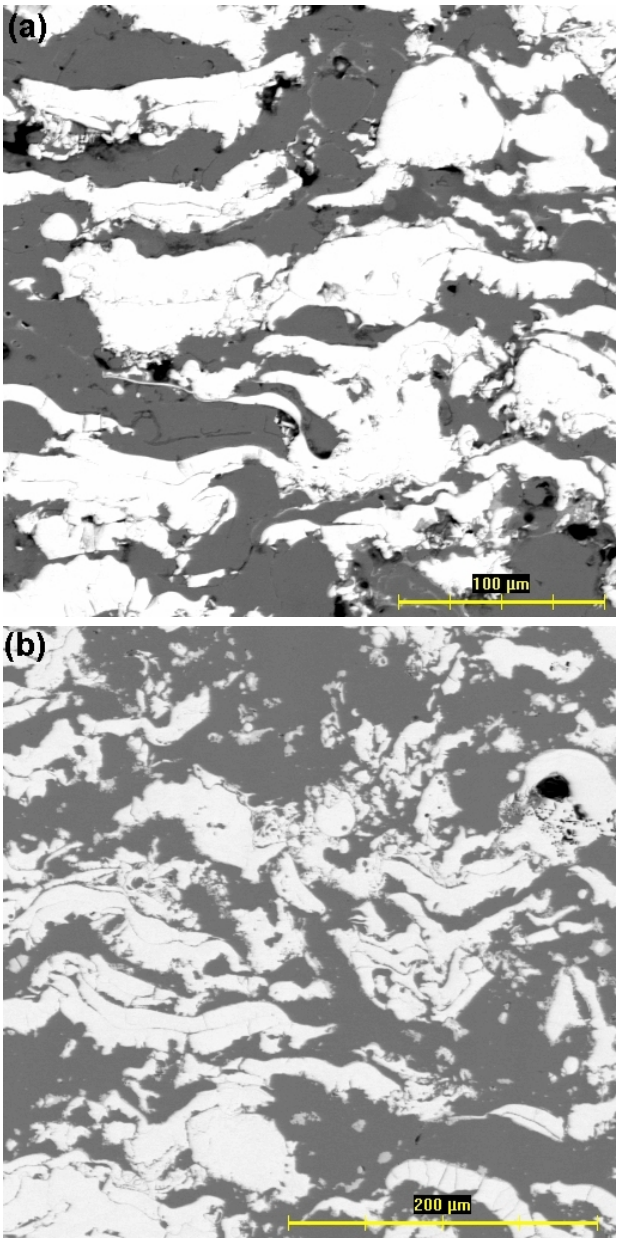

Figure 4. Structures of plasma sprayed 50/50 $W^{+}Cu$ composite in the a) as-sprayed and b) HIPped condition, showing a reduction in porosity and unbonded interfaces.

The breeding blanket will consist of the first wall, a neutron multiplier, a tritium breeding material, one or several coolants and a structural material to separate and contain the other materials [1, 87]. The exact form and composition of these components will depend on specific design concepts, which are still under development. These could be divided into two major directions: liquid metal breeder, where Pb-Li alloy (e.g. the eutectic Pb-16Li) serves as tritium breeder and neutron multiplier, and solid/ceramic breeder, where Li_4SiO_4 or Li_2TiO_3 pebble beds function as tritium breeder and Be as the neutron multiplier. In ITER, these concepts will be tested in the form of six test blanket modules (TBMs) installed in three

dedicated equatorial ports. The specific configurations are: Helium Cooled Lithium Lead (HCLL), Helium Cooled Pebble Bed (HCPB), Water Cooled Ceramic Breeder (WCCB), Dual Coolant Lithium Lead (DCLL), Helium Cooled Ceramic Breeder (HCCB) and Lithium Lead Ceramic Breeder (LLCB) [24]. According to simulations, the liquid metal blanket should have a higher TBR [13]. The first wall will be integrated with the blanket, therefore, its optimization will have to be done not only with regards to plasma performance but also blanket functions. For example, its thickness will directly affect the TBR, and therefore will have to be limited to a few mm or less [87]. The first wall of the TBMs will still act as a plasma facing component, although it will be recessed with respect to the other ITER first wall modules, in order to avoid major heat loads transients which are expected in ITER but should not to be present in DEMO [24]. While the ITER TBMs will represent only a small fraction of the plasma facing surface, in DEMO, the blanket will represent almost all of it.

Electrically insulating coatings, introduced in Section 4.5, will have an important function in the blanket as well, but in this case, the requirements are more complex. Electrical insulation is necessary for the liquid metal blankets, otherwise, the magnetic field acting on the flowing metal would induce electrical currents if the potential drop is short-circuited by the ducts. The resulting magnetohydrodynamic drop (MHD), in turn, would hinder the liquid flow and impart large mechanical stresses on the duct walls [58]. In this application, the coatings would have to serve as electrical insulators, corrosion and permeation barriers [49]. The MHD pressure drop strongly depends on the coating resistance; for proper insulation, the product of resistivity and thickness should be $>100\,\Omega\,\mathrm{cm}^2$ [11]. Similarly to tritium permeation barriers, the insulating capability is influenced by the presence of defects such as cracks [11]. Therefore, dense, contiguous and/or self-healing coatings are desirable. Oxides and nitrides are the prime candidates [81]. Only a few of these, however, are stable in liquid Li because it is a highly reducing agent. From the thermodynamic viewpoint, CaO, Y_2O_3, Er_2O_3 and AlN are expected to be stable in Li, as their free energy of formation is lower than Li_2O or Li_3N, respectively. For Al_2O_3 and $MgAl_2O_4$, these are comparable [58]. Al_2O_3, Y_2O_3, and Er_2O_3 have similar thermal expansion to V alloys, whereas the difference is larger for AlN. All of these have been researched as coatings for potential application in a breeding blanket. The production techniques studied include in situ formation during exposure of V alloys to lithium with controlled chemistry, various vapor deposition processes, pre-aluminization of the substrate followed by oxidation or nitridation, and plasma spraying [49]. Apart from the criteria mentioned above, the ability to coat internal surfaces is an important factor for the suitable technique selection.

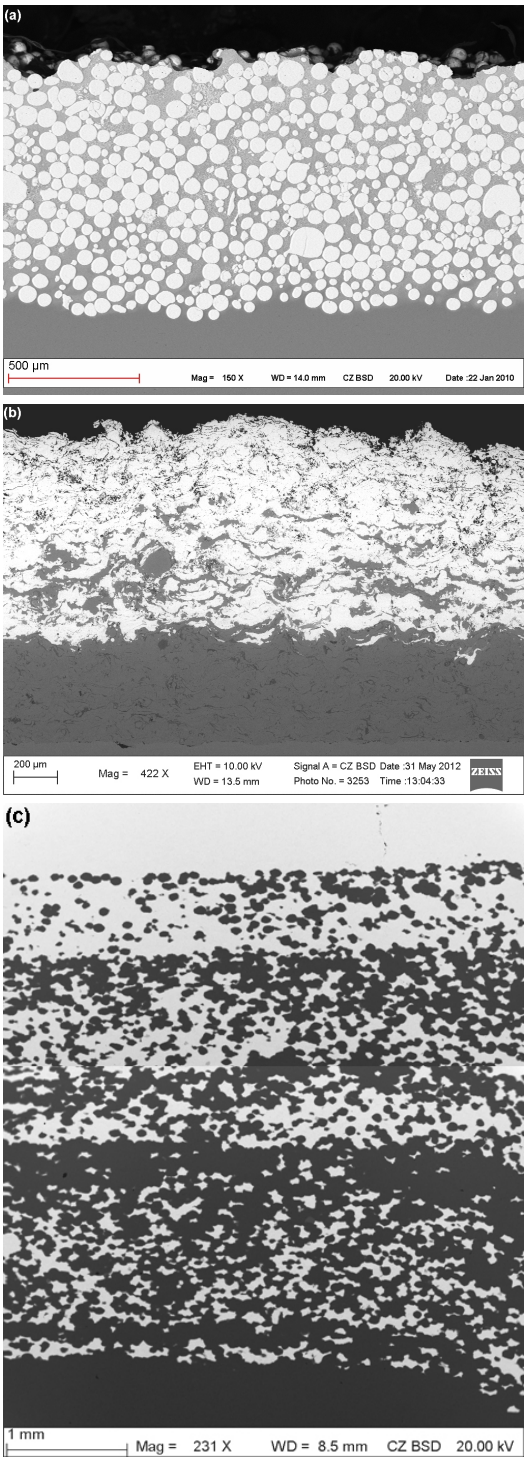

FIGURE 5. Examples of W+steel FGMs produced by a) laser cladding, b) water stabilized plasma spraying, c) hot pressing.

5. DEMO and New Developmental Materials

DEMO will be the demonstration fusion reactor aiming at electricity production, the next step on the development path towards commercial power produc-

tion. While the physical parameters of the plasma will not be dramatically different from ITER, there are significant differences in requirements on fusion power, lifetime of plasma-facing components and reliability of operation, besides large doses of irradiation [79, 8, 86]. The fusion power will increase roughly by an order of magnitude from ITER to DEMO and future commercial reactors without significant change in machine size [87]. Moreover, ITER will operate in pulsed mode, with relatively short pulses compared to the quasi-continuous or steady state operation expected in DEMO [24]. There will be smaller margin for accommodating off-normal thermal loads, therefore, the occurrence of large off-normal events will have to be restricted [67].

RAF and RAFM – reduced activation ferritic and ferritic/martensitic steels are considered to be the most promising structural materials for first wall and breeding blanket applications in future fusion reactors. They represent a good alternative to austenitic steels thanks to their much lower activation, higher swelling resistance, lower damage accumulation and improved thermal properties. However, their temperature usage window is roughly $350 \div 500\,^{\circ}\mathrm{C}$, the lower value being limited by irradiation-induced embrittlement effects (increase in DBTT) and the upper limit by a strong decrease in mechanical strength [3]. Generally, the RAF steels exhibit better high-temperature tensile and creep strengths than RAFM steels, but higher DBTT [2]. Addition of Ta and W alloying elements was found to increase fatigue life and reduce the degree of softening [76].

The temperature window can be significantly extended upwards (to about $750\,^{\circ}\mathrm{C}$) by using oxide dispersion strengthening (ODS) [66, 88]. In the ODS steels, a dispersion of fine thermally stable oxide particles is introduced by powder metallurgy/mechanical alloying and the powder is consolidated by hot isostatic pressing. Typically, from 0.2 to 0.4 wt% of Y_2O_3 or Y−Ti complex oxides of a few nm in size are used [88, 38]. These oxide particles serve as pinning sites hindering dislocation movement, thereby strengthening the material. Besides the oxide dispersion, a fine grain structure (∼µm) is also important. In the unirradiated state, the ODS EUROFER shows about 50 % higher yield strength and ultimate tensile strength compared to EUROFER 97, and a superior creep strength as well [2]. The applications foreseen for the ODS EUROFER include the plate supporting the tungsten tiles in the European dual coolant lithium-lead (DCLL) breeding blanket concept and the cartridge within the finger-like parts of the European He-cooled divertor concept (see below) [66].

Besides the RAF or RAFM steels, two classes of construction materials with a more developmental nature are considered: vanadium alloys and SiC/SiC composites. The motivation lies mainly in the much lower radioactivity [54], as well as the extension of usability temperature range, as higher temperatures permit increased energy conversion efficiency [87].

V-alloys are attractive because of their low activation, fast decay of activity and radiation resistance. On the other hand, they feature high solubility and permeability of tritium, solubility of interstitial impurities (O, C, N), easy oxidation and sensitivity of properties to the presence of these impurities. For example, oxidation of V-alloy can deteriorate its mechanical property even at 300 ppm oxygen [87]. Therefore, surface coatings acting as diffusion barriers for hydrogen isotopes and impurities are being developed [12, 45]. Among the critical issues are also the compatibility with Li and the mechanical property degradation of the alloy after Li exposure with or without neutron irradiation [12].

SiC−SiC composites, consisting of continuous SiC fiber-reinforced SiC-matrix, produced by chemical vapor infiltration or by nano-infiltration and transient eutectic-phase (NITE) process, also have a number of attractive characteristics. These are namely the ability to operate at temperature much higher than for metallic alloys (high strength is retained up to $1500\,^{\circ}\mathrm{C}$), very low radioactivity and high tolerance against neutron irradiation up to high temperatures, high corrosion resistance (or generally, chemical inertness), low density, high stiffness and low coefficient of thermal expansion [35]. On the other hand, this material is difficult to join; low activation glass-ceramics are being developed for this purpose [21]. A summary of properties of candidate structural materials for DEMO (RAF steels, V alloys, SiC and W) can be found in [87].

For the plasma facing components, tungsten is proposed as the main material [8, 97], particularly because of its low erosion and tritium retention. For the first wall, heat flux about $0.5\,\mathrm{MW\,m^{-2}}$ is expected. The thickness of the W armor will be in the order of mm, being a compromise between the considerations of erosion lifetime, tritium breeding, thermal stress and temperature of the underlying steel structure [31, 74, 8]. For the divertor, where a heat flux about $10\,\mathrm{MW\,m^{-2}}$ is foreseen, several concepts are being evaluated, either based on water or gas cooling. Water cooling has the advantage of high heat removal capability, while gas cooling can be performed at higher temperatures, resulting in a better thermal energy conversion efficiency [68]. Among the design concepts, the general idea is to distribute the heat load as uniformly as possible through the divertor [1]. The reference concept of He-cooled modular divertor with multiple-jet cooling (HEMJ) includes a series of small fingers – heat sinks – made of steel (e.g. the ODS EUROFER 97) and actively cooled with helium jets at high pressure. These would be covered with a thimble made of tungsten-based alloy and armored with a tungsten tile as the plasma facing surface. The cooling fingers would be connected

to the main structure by brazing in combination with a mechanical interlock [59].

For tungsten-steel joining in the first wall region, FGMs produced by various techniques are being explored. Examples of structures produced by laser cladding, plasma spraying by argon-water torch and hot pressing are shown in Fig. 5. The laser cladding technique succeeded to produce very dense composites of $1 \div 3$ mm thickness, with reasonable area coverage and minimal heat input to the base material, but failed to achieve a dense, full-W layer on the surface [69]. The characteristics of plasma spraying were already discussed in Section 4.4. The hot pressing technique again produced dense composites as well as full FGMs of ∼mm thickness [48]. Relatively small lateral size of the products presents a handicap with respect to large area coverage. Formation of Fe_7W_6 intermetallic compound was observed at the steel/W interface, caused by the high temperature exposure (2000 °C in this case). The relatively brittle nature of this compound may undermine the overall strength of the composite. When a third material (tungsten carbide) was applied to separate the steel and tungsten, as suggested in [56], another phase, consisting of Fe, W and C, formed at the interface. This may be avoided by reducing the processing temperature (e.g. by using spark plasma sintering), but these phases may appear nevertheless during prolonged exposure to higher temperatures in service.

For a plasma facing material, an alternative to the high-melting-point materials could be a flowing liquid metal. Flowing liquids have high heat load capability (up to about $50\,\mathrm{MW\,m^{-2}}$) and could provide simultaneous heat and particle removal. The liquids being considered are lithium, gallium, tin, lithium-tin mixture and molten salt mixture of LiF and BeF_2 (commonly called FLIBE). The issues to be tackled include magnetohydrodynamic effects on flowing conducting liquids, corrosion, erosion and dust and practical realization (e.g. a capillary porous system) [1, 53, 75].

6. Conclusions

Successful realization of nuclear fusion as a source of energy is critically dependent on the development of suitable materials. The components of a fusion reactor will have to function in extremely harsh environment, and thus the requirements for materials and design are very complex. Solutions to the present problems cannot be provided by new/improved materials alone, but require strong interaction and cooperation among experts in the fields of materials science, technology, plasma physics and plasma control.

Acknowledgements

This work, partially supported by the European Communities under the contract of Association between EURATOM and IPP.CR, was carried out within the framework of the European Fusion Development Agreement (task no. WP11-MAT-WWALLOY). The views and opinions expressed herein do not necessarily reflect those of the European Commission. Partial support through the Institutional Research Plan no. AV0Z20430508, Czech Ministry of Education, Youth and Sports grant no. 7G10072 and Czech Science Foundation grant no. P108/12/1872 is also acknowledged.

References

[1] N. Baluc. Materials for fusion power reactors. *Plasma Phys Controlled Fusion* **48**(12B):B165–B177, 2006.

[2] N. Baluc. Material degradation under DEMO relevant neutron fluences. *Phys Scr* **T138**:014004, 2009.

[3] N. Baluc, et al. On the potentiality of using ferritic/martensitic steels as structural materials for fusion reactors. *Nucl Fusion* **44**(1):56–61, 2004.

[4] V. Barabash, et al. Armor and heat sink materials joining technologies development for Iter plasma facing components. *J Nucl Mater* **283**:1248–1252, 2000.

[5] V. Barabash, et al. Material/plasma surface interaction issues following neutron damage. *J Nucl Mater* **313**:42–51, 2003.

[6] B. Bazylev, et al. Behaviour of melted tungsten plasma facing components under Iter-like transient heat loads simulations and experiments. *Fusion Eng Des* **83**(7–9):1077–1081, 2008.

[7] H. Bolt, et al. Plasma facing and high heat flux materials – needs for ITER and beyond. *J Nucl Mater* **307**:43–52, 2002.

[8] H. Bolt, et al. Materials for the plasma-facing components of fusion reactors. *J Nucl Mater* **329**:66–73, 2004.

[9] R. A. Causey, et al. The effects of neutron damage on the retention of tritium in carbon composites. *Phys Scr* **T64**:32–35, 1996.

[10] R. A. Causey, et al. *Tritium barriers and tritium diffusion in fusion reactors*. Elsevieer, 2012. Edited by Konings, R. J. M.

[11] H. Chen, et al. Insulating performance requirements for the coating material in the ITER DFLL electromagnetic TBM based on the MHD analysis. *J Nucl Mater* **386-88**:904–907, 2009.

[12] J. M. Chen, et al. Overview of the vanadium alloy researches for fusion reactors. *J Nucl Mater* **417**(1-3):289–294, 2011.

[13] B. R. Colling, S. D. Monk. Development of fusion blanket technology for the DEMO reactor. *Appl Radiat Isot* **70**:13701372, 2012.

[14] R. W. Conn, et al. Beryllium as the plasma-facing material in fusion energy systems – experiments, evaluation, and comparison with alternative materials. *Fusion Eng Des* **37**(4):481–513, 1997.

[15] Y. Dai, et al. *The effects of helium in irradiated structural alloys*. Elsevieer, 2012. Edited by Konings, R. J. M.

[16] J. W. Davis, et al. Assessment of tungsten for use in the ITER plasma facing components. *J Nucl Mater* **263**:308–312, 1998.

[17] M. Decreton, et al. Performance of functional materials and components in a fusion reactor: the issue of radiation effects in ceramics and glass materials for diagnostics. *J Nucl Mater* **329**:125–132, 2004.

[18] J. Du, et al. Interfacial fracture behavior of tungsten wire/tungsten matrix composites with copper-coated interfaces. *Materials Science and Engineering A* **527**(6):1623–1629, 2010.

[19] International Fusion Materials Irradiation Facility. `http://www.ifmif.org`.

[20] G. Federici, et al. *Beryllium as a plasma-facing material for near-term fusion devices*. Elsevieer, 2012. Edited by Konings, R. J. M.

[21] M. Ferraris, et al. Joining of SiC-based materials for nuclear energy applications. *J Nucl Mater* **417**(1-3):379–382, 2011.

[22] M. Fujitsuka, et al. Effect of neutron irradiation on thermal diffusivity of tungsten-rhenium alloys. *J Nucl Mater* **283**:1148–1151, 2000.

[23] Magnetic Fusion. Tritium breeding blankets. `http://www-fusion-magnetique.cea.fr/gb/cea/next/couvertures/blk.htm`.

[24] L. M. Giancarli, et al. Overview of the ITER TBM program. *Fusion Eng Des* 2012. In press.

[25] A. A. Haasz, J. W. Davis. Hydrogen isotopic effects on the erosion of carbon. *Fusion Science and Technology* **50**(1):58–67, 2006.

[26] A. Hassanein. Prediction of material erosion and lifetime during major plasma instabilities in tokamak devices. *Fusion Eng Des* **60**(4):527–546, 2002.

[27] J. B. J. Hegeman, et al. Mechanical and thermal properties of SiC(f)/SiC composites irradiated with neutrons at high temperatures. *Fusion Eng Des* **75–79**:789–793, 2005.

[28] T. Hirai, et al. Failure modes of vacuum plasma spray tungsten coating created on carbon fibre composites under thermal loads. *J Nucl Mater* **392**(1):40–44, 2009.

[29] E. R. Hodgson, T. Shikama. *Radiation effects on the physical properties of dielectric insulators for fusion reactors*. Elsevieer, 2012. Edited by Konings, R. J. M.

[30] K. J. Hollis, et al. Plasma-sprayed beryllium on macro-roughened substrates for fusion reactor high heat flux applications. *Journal of Thermal Spray Technology* **16**(1):96–103, 2007.

[31] Y. Igitkhanov, B. Bazylev. Evaluation of energy and particle impact on the plasma facing components in DEMO. *Fusion Eng Des* **87**(5–6):520–524, 2012.

[32] ITER. http://www.iter.org.

[33] R. K. Janev, A. Miyahara. Plasma material interaction issues in fusion-reactor design and status of the database. *Nucl Fusion* **1**:123–138, 1991.

[34] Y. I. Jung, et al. Ion-beam assisted deposition of coating interlayers for the joining of Be/CuCrZr. *Fusion Eng Des* **85**(7-9):1689–1692, 2010.

[35] Y. Katoh, et al. Current status and critical issues for development of SiC composites for fusion applications. *J Nucl Mater* **367**:659–671, 2007.

[36] F. Koch, et al. Crystallization behavior of arc-deposited ceramic barrier coatings. *J Nucl Mater* **329**:1403–1406, 2004.

[37] F. Koch, et al. Oxidation behaviour of silicon-free tungsten alloys for use as the first wall material. *Phys Scr* **T145**:014019, 2011.

[38] I. Kuběna, et al. Effect of microstructure on low cycle fatigue properties of ODS steels. *J Nucl Mater* **424**(1-3):101–108, 2012.

[39] K. J. Leonard. *Radiation effects in refractory metals and alloys*. Elsevieer, 2012. Edited by Konings, R. J. M.

[40] C. Linsmeier, et al. Mixed material formation and erosion. *J Nucl Mater* **290**:25–32, 2001.

[41] M. Lipa, et al. The use of copper alloy CuCrZr as a structural material for actively cooled plasma facing and in vessel components. *Fusion Eng Des* **75-79**:469–473, 2005.

[42] P. Lopez-Ruiz, et al. Self-passivating bulk tungsten-based alloys manufactured by powder metallurgy. *Phys Scr,* **T145**:014018, 2011.

[43] H. Maier. Tungsten erosion in the baffle and outboard regions of the ITER-like ASDEX upgrade divertor. *J Nucl Mater* **335**(3):515–519, 2004.

[44] R. Matera, G. Federici. Design requirements for plasma facing materials in ITER. *J Nucl Mater* **233–237**:17–25, 1996.

[45] S. Mathieu, et al. Multi-layered silicides coating for vanadium alloys for generation IV reactors. *Surf Coat Technol* **206**:4594–4600, 2012.

[46] Matějíček, R. J., Mušálek. *Processing and properties of plasma sprayed W+Cu composites*. DVS Verlag, Dusseldorf, 2008. Edited by Lugscheider, E.

[47] J. Matějíček, et al. Methods of increasing thermal conductivity of plasma sprayed tungsten-based coatings. *Advanced Materials Research* **59**:82–86, 2009.

[48] J. Matějíček, et al. Tungsten-steel composites and FGMs produced by hot pressing. In *21st International Conference on Metallurgy and Materials METAL 2012*. Tanger, Ostrava, 2012. Paper no. 177.

[49] J. Matějíček, P. Chráska. Development of advanced coatings for iter and future fusion devices. *Advances in Science and Technology* **66**:47–65, 2010.

[50] J. Matějíček, P. Chráska, J. Linke. Thermal spray coatings for fusion applications-review. *Journal of Thermal Spray Technology* **16**(1):64–83, 2007.

[51] J. Matějíček, Y. Koza, V. Weinzettl. Plasma sprayed tungsten-based coatings and their performance under fusion relevant conditions. *Fusion Eng Des* **75-79**:395–399, 2005.

[52] P. J. Maziasz, J. T. Busby. *Properties of austenitic steels for nuclear reactor applications*. Elsevieer, 2012. Edited by Konings, R. J. M.

[53] G. Mazzitelli, et al. Heat loads on FTU liquid lithium limiter. *Fusion Eng Des* **86**(6-8):580–583, 2011.

[54] G. McCracken, P. Stott. *Fusion – the energy of the universe*. Elsevier Academic Press, Burlington, 2005.

[55] M. Merola, et al. Overview on fabrication and joining of plasma facing and high heat flux materials for ITER. *J Nucl Mater* **307**:1524–1532, 2002.

[56] J. M. Missiaen, et al. Design of a W/steel functionally graded material for plasma facing components of DEMO. *J Nucl Mater* **416**(3):262–269, 2011.

[57] A. Morono, E. R. Hodgson. Radiation induced conductivity and surface electrical degradation of plasma sprayed spinel for NBI systems. *Fusion Eng Des* **75–79**:1075–1078, 2005.

[58] T. Muroga, B. A. Pint. Progress in the development of insulator coating for liquid lithium blankets. *Fusion Eng Des* **85**(10):1301–1306, 2010.

[59] P. Norajitra, et al. Progress of He-cooled divertor development for Demo. *Fusion Eng Des* **86**(9-11):1656–1659, 2011.

[60] B. C. Odegard, et al. A review of the US joining technologies for plasma facing components in the ITER fusion reactor. *J Nucl Mater* **263**:329–334, 1998.

[61] O. V. Ogorodnikova, et al. Deuterium retention in tungsten in dependence of the surface conditions. *J Nucl Mater* **313**:469–477, 2003.

[62] J. Pamela, et al. An ITER-like wall for JET. *J Nucl Mater* **363**:1–11, 2007.

[63] G. Pintsuk. *Tungsten as a plasma-facing material*. Elsevieer, 2012. Edited by Konings, R. J. M.

[64] G. Pintsuk, et al. Development of W/Cu-functionally graded materials. *Fusion Eng Des* **66-68**:237–240, 2003.

[65] G. Pintsuk, et al. Fabrication and characterization of vacuum plasma sprayed W/Cu-composites for extreme thermal conditions. *J Mater Sci* **42**(1):30–39, 2007.

[66] G. Pintsuk, et al. High heat flux testing of 12-14Cr ODS ferritic steels. *J Nucl Mater* **396**(1):20–25, 2010.

[67] A. R. Raffray, et al. High heat flux components-readiness to proceed from near term fusion systems to power plants. *Fusion Eng Des* **85**(1):93–108, 2010.

[68] J. Reiser, M. Rieth. Optimization and limitations of known DEMO divertor concepts. *Fusion Eng Des* **87**(5–6):718–721, 2012.

[69] M. Rieth, et al. Recent progress on tungsten materials research for nuclear fusion applications in Europe. *J Nucl Mater* **432**:482–500, 2013.

[70] M. Rosinski, et al. W/Cu composites produced by pulse plasma sintering technique (PPS). *Fusion Eng Des* **82**(15-24):2621–2626, 2007.

[71] J. Roth, et al. Tritium inventory in ITER plasma-facing materials and tritium removal procedures. *Plasma Phys Controlled Fusion* **50**(10):103001, 2008.

[72] J. Roth, et al. Recent analysis of key plasma wall interactions issues for ITER. *J Nucl Mater* **390–91**:1–9, 2009.

[73] J. Roth, K. Schmid. Hydrogen in tungsten as plasma-facing material. *Phys Scr* **T145**:014031, 2011.

[74] S. Sato, et al. Experimental studies on tungsten-armour impact on nuclear responses of solid breeding blanket. *Nucl Fusion* **45**(7):656–662, 2005.

[75] F. Scaffidi-Argentina, et al. The status of beryllium technology for fusion. *J Nucl Mater* **283**:43–51, 2000.

[76] V. Shankar, et al. Effect of tungsten and tantalum on the low cycle fatigue behavior of reduced activation ferritic/martensitic steels. *Fusion Eng Des* **87**(4):318–324, 2012.

[77] T. Shikama, et al. Irradiation effects in ceramics for fusion reactor applications. *J Nucl Mater* **271**:560–568, 1999.

[78] T. Shikama, S. J. Zinkle. Electrical in situ and post-irradiation properties of ceramics relevant to fusion irradiation conditions. *J Nucl Mater* **307**:1073–1079, 2002.

[79] Y. Shimomura. ITER and plasma surface interaction issues in a fusion reactor. *J Nucl Mater* **363**:467–475, 2007.

[80] I. Smid, et al. Development of tungsten armor and bonding to copper for plasma-interactive components. *J Nucl Mater* **263**:160–172, 1998.

[81] D. L. Smith, et al. Development of coatings for fusion power applications. *J Nucl Mater* **307**:1314–1322, 2002.

[82] L. L. Snead, et al. Thermal conductivity degradation of ceramic materials due to low temperature, low dose neutron irradiation. *J Nucl Mater* **340**(2–3):187–202, 2005.

[83] L. L. Snead, M. Ferraris. *Carbon as a fusion plasma-facing material*. Elsevieer, 2012. Edited by Konings, R. J. M.

[84] T. Tanabe. Tritium handling issues in fusion reactor materials. *J Nucl Mater* **417**(1-3):545–550, 2011.

[85] T. Terai. Research and development on ceramic coatings for fusion reactor liquid blankets. *J Nucl Mater* **248**:153–158, 1997.

[86] R. Toschi, et al. How far is a fusion power reactor from an experimental reactor. *Fusion Eng Des* **56-57**:163–172, 2001.

[87] Y. Ueda, et al. PSI issues at plasma facing surfaces of blankets in fusion reactors. *J Nucl Mater* **313**:32–41, 2003.

[88] S. Ukai. *Oxide dispersion strengthened steels*. Elsevieer, 2012. Edited by Konings, R. J. M.

[89] M. Vilémová, et al. Application of structure-based models of mechanical and thermal properties on plasma sprayed coatings. *Journal of Thermal Spray Technology* **21**(3-4):372–382, 2012.

[90] P. Vladimirov, A. Moslang. Comparison of material irradiation conditions for fusion, spallation, stripping and fission neutron sources. *J Nucl Mater* **329**:233–237, 2004.

[91] T. Weber, J. Aktaa. Numerical assessment of functionally graded tungsten/steel joints for divertor applications. *Fusion Eng Des* **86**(2-3):220–226, 2011.

[92] T. Weber, et al. Resistance sintering under ultra high pressure of tungsten/eurofer97 composites. *J Nucl Mater* **414**(1):19–22, 2011.

[93] Wikipedia. Edge localized mode. `http://en.wikipedia.org/wiki/Edge-localized_mode`.

[94] Wikipedia. Hydrogen embrittlement. `http://en.wikipedia.org/wiki/Hydrogen_embrittlement`.

[95] Wikipedia. Stellarator. `http://en.wikipedia.org/wiki/Stellarator`.

[96] Wikipedia. Tokamak. http://en.wikipedia.org/wiki/Tokamak.

[97] C. P. C. Wong. Innovative tokamak DEMO first wall and divertor material concepts. *J Nucl Mater* **390-91**:1026–1028, 2009.

[98] T. Yano, et al. Neutron irradiation damage in aluminum oxide and nitride ceramics up to a fluence of 4.2×10^{26} n/m^2. *J Nucl Mater* **283**:947–951, 2000.

[99] Z. Zhong, et al. *Diffusion bonding of tungsten to reduced activation ferritic/martensitic steel F82H using a titanium interlayer*. Springier Japan, 2010. Edited by Yao, T.

[100] S. J. Zinkle, C. Kinoshita. Defect production in ceramics. *J Nucl Mater* **251**:200–217, 1997.